rOi-Space: Accelerated imaging of sub-volumes using ROI focused O-Space

Kopanoglu E, Wang H, Wan Y, Peters DC, Galiana G, Constable RT
Diagnostic Radiology, Yale University, New Haven, CT, USA

Target Audience

Researchers interested in accelerated imaging, sub-volume imaging and nonlinear gradient fields.

Purpose

In conventional MRI, linear gradient fields (LGFs) are used for spatial encoding. However, recent years have shown increased attention to nonlinear gradient fields (NLGFs), owing to various advantages such fields offer including reduced RF power [1], curved slice imaging [2], locally enhanced resolution [3] and faster data acquisition [4]. O-Space imaging [4,5] relies on the Z2-harmonic $(x^2/2 + y^2/2 - z^2)$ and performs imaging by spatially shifting the center of this field using LGFs. Because the encoding field varies along all dimensions, oversampling during readout increases resolution in both dimensions in an axial image, enabling fewer pulse repetitions. Unless previous work on reduced-FOV imaging with NLGFs [6,7], this method provides an intuitive and simple approach based on a single gradient channel.
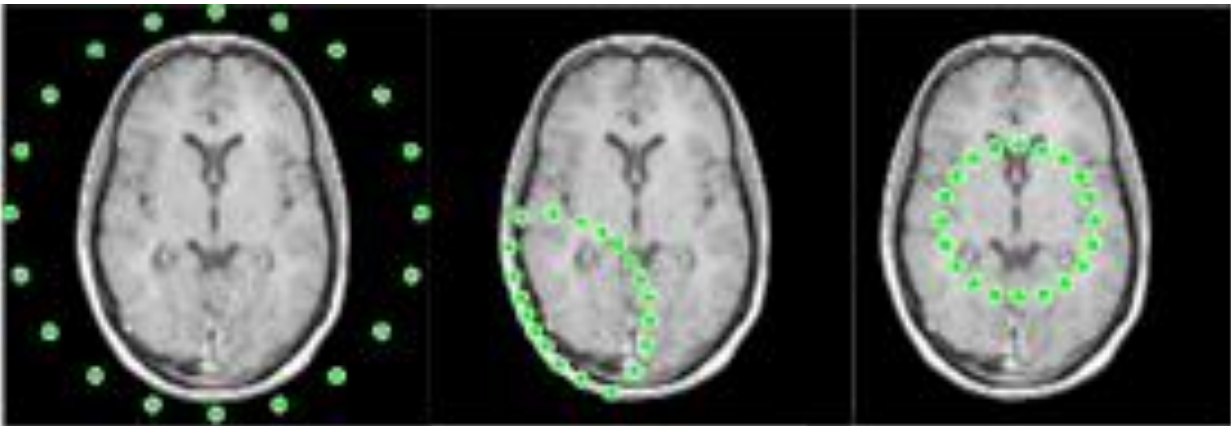

*Figure 1: Left: The center placements of the Z2-field are uniformly distributed on a circle that has a diameter equal to the FOV. **Middle & Right:** The center placements are distributed on the boundary of the ROI in rOi-Space imaging. Middle: South-West (SW) ROI. Right: Center-ROI.*

In this study, we propose a new O-Space imaging method, for imaging sub-volumes. In O-Space, the center of the Z2 field is shifted to equidistant points lying on a circle that has a diameter equal to the field-of-view (FOV) whereas here, we propose placing the center of the Z2-field on the boundary of the region-of-interest (ROI) to increase the encoding performance inside the ROI (Figure 1), hence the name of the method, rOi-Space.
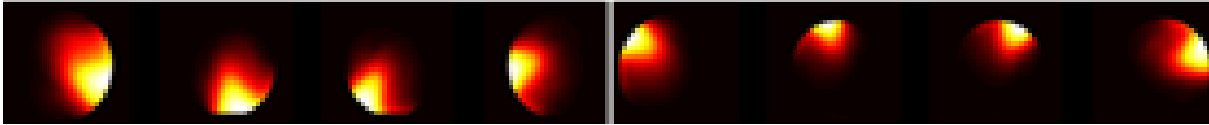
Figure 2: *Magnitude-wise coil sensitivities of the 8-ch receive coil (phase distributions not shown here for simplicity).*
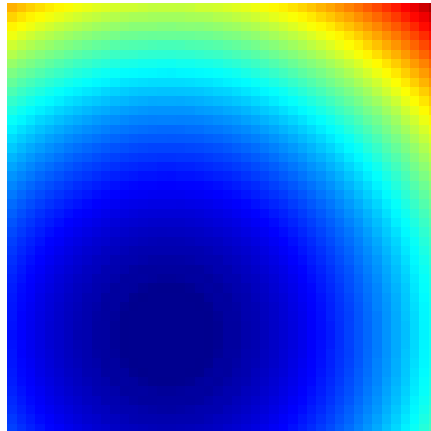

Figure 3: *The field distribution of the Z2-field when the center is shifted using LGFs.*

Methods

Simulations were performed in Matlab (Mathworks Inc., Natick, MA, USA). Simulation parameters were; spatial resolution, 200×200; FOV, $(20\ cm)^2$; bandwidth, 40Hz/px; number of readout points, 512. Images were reconstructed using the Algebraic Reconstruction Technique with 5 iterations and $\lambda = 0.75$. In the simulations, experimentally obtained sensitivity profiles from an 8-channel head-coil (Figure 2) were used [8]. The spatial encoding functions generated by the gradient fields (Figure 3) were averaged over a 5×5 higher resolution grid to incorporate intra-voxel dephasing effects (sufficient for the field strengths used).

The first ROI (SW: South-West) was determined to be the intersection of the object and a circular region (radius: $FOV/4$) centered at $(x, y) = (-FOV/4, -FOV/4)$ and the second ROI was circular (radius: $FOV/6$) and centered at the origin (Figure 1). For rOi-Space, the center of the Z2 field was placed at the intersection of the ROI boundary with radial rays originating from the center of the ROI that are equally apart angular-wise. The number of center placements tested was between 10 and 35 and the methods were compared in terms of root-mean-squared-error (RMSE).

Because the Z2-field varies slowly around its center, only low-frequency information is obtained from the spins near the center, whereas regions off-center experience the sharpest gradients. Therefore, moving the CPs closer to the ROI reduces the bandwidth of the signal received from the ROI. To compensate for this reduction, the NLGF amplitude was increased from a typical 10 mT/m² to 40 mT/m². To make a fair comparison to O-Space, its performance was evaluated at both field strengths for the SW-ROI whereas a similar comparison was omitted for the center-ROI for conciseness.
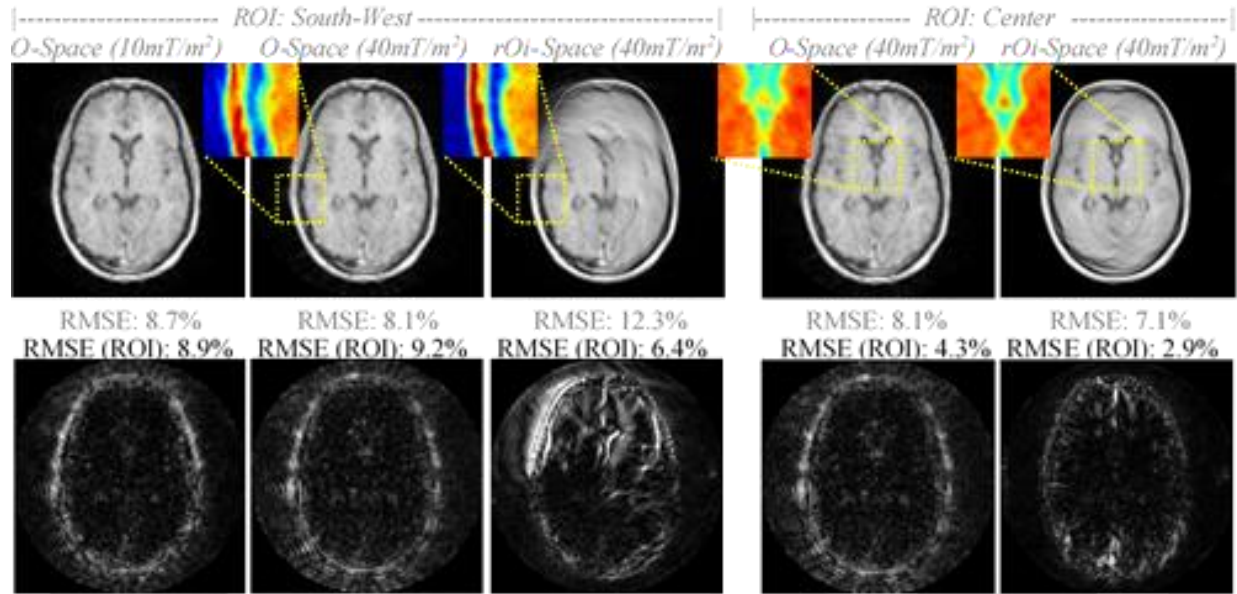
Figure 4: 1st row: *Comparison of O-Space and rOi-Space images for both ROIs (SW and center). The colored insets show magnified regions for comparison.* **2nd row:** *Difference images between the obtained and the actual images were magnified four-times to increase clarity.* **3rd row:** *Comparison of RMS-error inside the ROI and the reduction obtained using rOi-Space. 20 center-placements were used in all cases.*

Results

The difference images in Figure 4 show fairly uniform spatial variations across the FOV for O-Space whereas for rOi-Space the artifacts are more pronounced outside the ROIs, and less so inside the ROIs. On average, the proposed method reduced the RMSE by 22% and 29% for the SW-ROI compared to O-Space with $10mT/m^2$ and $40mT/m^2$ NLGF amplitudes, respectively and by 23% for the center-ROI whereas for the given images (20 center-placements), the reductions were 28% and 30% for the SW-ROI and 33% for the center-ROI. The colored insets demonstrate that the proposed method increases sharpness inside the ROI. Note that these simulations were noise-free to highlight the difference between the methods. When noise was incorporated, rOi-Space again yielded improved results; for the SW-ROI case with 20 CPs, the RMSE increased to 10.2% and 15.1% for rOi-Space and O-Space, respectively, yielding 33% less RMSE for rOi-Space.

Discussion

Because O-Space encodes spatial information along both transverse dimensions in every TR, it provides acceleration factors that may exceed the number of available received coils [9]; Figure 4 shows images obtained with only 20 center placements and 8-coils, for a reconstructed resolution of 200×200. However, O-Space images the whole FOV. The proposed method improves the accelerated imaging performance of O-Space further by focusing the encoding effort to the ROI. The examples provided showed that for similar RMSE values, rOi-Space may reduce scan time by 25% on average, compared to O-Space.

Conclusion

The proposed method reduces the scan-time of the accelerated-imaging method O-Space for cases where the region-of-interest is a sub-volume of the subject. Possible application areas that are currently under investigation include cardiac imaging.

Acknowledgments

References

1. Kopanoglu E *et al.* MRM 2013;70(2):537-546.
2. Weber H *et al.* MRM 2013;69(5):1317-1325.
3. Hennig J *et al.* MAGMA 2008;21(1-2):5-14.
4. Stockmann JP *et al.* MRM 2010;64(2):447-456.
5. Stockmann JP *et al.* MRM 2013;69(2):444-455.
6. Witschey WRT *et al.* MRM 2012;67(6):1620-1632.
7. Layton KJ *et al.* MRM 2013;70(3):684-696.
8. Walsh DO *et al.* MRM 2000;43(5):682-690.
9. Tam LK *et al.* ISMRM, Milan, Italy, p. 1559, 2014.